Stochastic Models in Risk-based Assessment of Reserve Requirements for a Power System with High Wind Power Generation

Michael Negnevitsky
School of Engineering and ICT
University of Tasmania
Hobart, TAS 7000, Australia
Michael.Negnevitsky@utas.edu.au

Dinh Hieu Nguyen
School of Engineering and ICT
University of Tasmania
Hobart, TAS 7000, Australia
hieu.nguyen@utas.edu.au

Marian Piekutowski
Hydro Tasmania
Hobart TAS 7000, Australia
marian.piekutowski@hydro.com.au

***Abstract*—The increasing role of wind power generation has created new challenges in power system planning and operation. Uncertainty of wind energy may lead to significant load-generation imbalances resulting in large frequency deviations, and hence increase system operation risk. Large wind penetration may also deteriorate the system primary frequency response due to its limited contribution to both system inertia and frequency control under the current practice of determining primary reserve. This paper proposes a risk-based approach to the adequacy assessment of primary frequency response. It can also assist in determining primary reserves requirements for a power system with significant penetration of wind power generation. A simplified dynamic model of frequency taking into account the system inertia and frequency control services is developed for fast evaluation of operational risks due to inadequate frequency response without performing dynamic simulations.**

Keywords – primary frequency response, reserve requirements, risk assessment, wind power generation

I. INTRODUCTION

In their attempt to reduce greenhouse-gas emissions from electric power industry and deal with diminishing natural resources, many countries are increasing their use of renewable energy sources, particularly wind power generation (WPG). Wind energy is a variable resource with limited availability that changes in time (variability), and despite significant improvement of wind power forecasting it cannot be accurately predicted (uncertainty). At some stages, the variability and uncertainty may lead to significant load-generation imbalances resulting in large frequency deviations, which in turn, may cause unwanted load shedding (or, in some cases, lead to a system black-out).

In addition, modern WPG units, particularly electronic converter-based variable-speed wind turbines, have different mechanisms for regulating their output and reacting to changes associated with voltage or frequency disturbances, compared to conventional thermal and hydropower generating units. Firstly, the moving parts of a wind turbine are not synchronized with the system frequency. As a result, the kinetic energy stored in a wind turbine is independent of system frequency. In other words, the contribution of a wind turbine to the system inertia is limited. Secondly, since wind turbines are normally operated to extract maximum power from wind (while wind is an uncontrollable energy source), wind turbines power output cannot be increased in response to a frequency drop like the output from synchronous generators equipped with governors. Thus, the integration of wind power will reduce the average system inertia and governor ramping capability per unit of installed capacity. Especially, if this integration results in the decommissioning of conventional power plants, it will reduce the total system inertia and governor ramping capability significantly, leading to lower frequency nadirs and higher rate of change of frequency (RoCoF). This may cause unwanted load curtailment due to under-frequency load-shedding and trip of generators triggered by their RoCoF protection relays.

Moreover, during low voltage ride through (LVRT) operation, wind turbines rapidly reduce active power production in order to inject additional reactive power into the grid. If a frequency disturbance is accompanied by depressed system voltage, WPG output is significantly reduced for a short period of time (from about 0.5s to 3s), which increases the magnitude of the frequency excursion [1]. For example, in a small power system, a forced outage of a large generator may lead to a large frequency deviation as well as drawing the voltage throughout the network down. As a result, wind turbines in the network reduce active power output during the fault proportionally to the voltage drop at their terminals due to LVRT operation. This reduction dramatically increases both the RoCoF and the magnitude of frequency nadir (the minimum *frequency*), and hence may lead to under-frequency load-shedding. Detailed description of this phenomenon can be found in [2].

Therefore, large wind penetration may reduce the adequacy of system frequency responses especially primary frequency responses. The adequacy of frequency responses is defined as the capability of power system reserves to prevent frequency from dropping below a certain limit [3]. It may also deteriorate the current practices used for determining operating reserves under low system inertia and insufficient number of machines providing frequency control, especially in small and isolated power systems.

978-1-4673-9941-8/16 $31.00 © 2016 IEEE
DOI 10.1109/SMRLO.2016.32

Operating reserve requirements are generally set using the deterministic criteria based on the size of the largest online infeed and may remain constant for all operating conditions during the year. However, recent studies [4]-[6] proposed that operating reserve requirements need to be set dynamically to cope better with the uncertain characteristics of a power system including wind generation variability and uncertainty. In [7], the author studied the impact of WPG on primary, secondary and tertiary reserves, and concluded that these reserve requirements increase proportionally to the installed WPG capacity. However, this conclusion does not take into account the cost and ability to provide additional reserves. Persaud *et al.* [8] concluded that the spinning reserve requirements are inversely proportional to the net demand (load minus WPG) forecasting accuracy. Therefore, when WPG is integrated to a power system, larger amounts of reserve would be required to maintain the same level of system security. However, this conclusion is based on the assumption that the reserve requirement is set based on a predefined security index, and hence the authors do not consider the balance that should be attained between costs of and benefits of spinning reserves for an efficient economic operation. Doherty and O'Malley [9] proposed to set spinning reserve requirements based on a predefined minimum system reliability level considering the installed wind capacity. However, setting a single level of reliability to be achieved at all periods of the optimization horizon results in suboptimal solutions as the cost and benefit of the reserve provision depends on several factors such as system demand, WPG output and units committed. In [10], the authors considered the wind forecast uncertainty and set the reserve requirements at 3.5 times of the standard deviation of the net demand error to capture more than 99.7% of system imbalances. However, this approach ignores the probability and extent of the system's contingencies and simply set larger amounts of spinning reserves as the total WPG production increases.

Ortega-Vaquez and Kirschen [6], [11] proposed a probabilistic method to estimate the optimal spinning reserve requirements and operating costs in a power system with significant WPG. Probabilistic techniques are also used in [5], [12] to determine system reserve requirements for wind power integration. Using probabilistic methods and stochastic programming, Bouffard and Galiana [4] presented a short-term forward electricity market-clearing problem with stochastic security for operation planning capable of accounting for wind power generations. A probabilistic framework for optimal reserve scheduling and N-1 secure daily dispatch of systems with significant wind power is proposed in [13]. It is generally agreed that a large-scale integration of WPG will result in an increase in the required amount of operating reserves to maintain system reliability. System operators should use the available information to estimate the system operating risk, and then schedule operating reserves accordingly.

However, most of these studies mainly focus on the steady state behaviour of the secondary and tertiary frequency control to estimate the expected social cost of load interruptions due to insufficient operating reserves. None of them consider the dynamic primary frequency response when determining the reserve requirement. These studies assume that the impact of large-scale WPG integration on primary reserve requirements and performance is negligible [4]-[6], [12]-[13]. While this assumption is usually valid in large systems with high inertia and primary control reserves, this may not be true in small and isolated power systems, which have low inertia and limited capabilities of providing fast primary control responses, due to the variability, uncertainty and asynchronism of WPG as explained previously.

This paper proposes a novel approach to evaluating the adequacy of primary frequency response (PFR) in a power system with significant wind power generation. This approach is based on the risk assessment method presented in our previous work [15]. Firstly, for fast evaluation of PFR adequacy without performing dynamic simulations a mathematical model of frequency trajectory in frequency excursion events is developed taking into account system inertia and frequency control services. The evaluated risk of primary frequency response inadequacy is then included in a security-constrained economic dispatch to determine the primary reserve requirement. The effectiveness of the proposed approach is illustrated by its application to a test system under different scenarios.

II. Dynamic Model of System Frequency

One of the main tasks in a power system is to maintain the balance between the electrical power produced by generators and the power consumed by loads, including system loses. If for some reasons such as load changes or generation variations this balance is not maintained, it will lead to a frequency excursion. A frequency drop could lead to increased magnetizing currents in induction motors and transformers. Large frequency excursions may also have serious impacts on the power system operation and the reliability of power supply. This section presents the development of mathematical models for system frequency trajectories in load-generation imbalance events.

Due to system uncertainties such as unplanned outages of network components and/or errors in load and WPG forecasts, an imbalance between load and generation can occur, leading to deviations in frequency. After a frequency deviation occurs, rotating machines in a power system immediately release their kinetic energy to arrest the change in frequency. This is called inertial response. The change in frequency can be expressed as follow [16]:

$$\frac{df}{dt} = \frac{f_0}{2\sum HS}\left(\Delta P_g - \Delta P_l\right) \quad (1)$$

where f is the system frequency, f_0 is the nominal frequency,

$\sum HS$ is the aggregate effective inertia of all rotating units in the system, ΔP_g and ΔP_l are the changes in generation and load from the steady state values, respectively.

Let us assume that the load-generation imbalance is caused by a sudden loss of generation "*g*" at time $t = 0$. As a result we have

$$\Delta P_g = -g$$
$$\Delta P_l = -kP_{l0}(1 - f/f_0) \quad (2)$$

where P_{l0} is the load level at frequency f_0 before the contingency occurs and k is the load relief factor.

Using the Laplace transformation technique for (1) and (2), the dynamic model of frequency can be expressed as

$$\varphi = \delta_g \left(e^{\frac{-t}{T_s}} - 1\right) \qquad \text{for } t \geq 0 \quad (3)$$

where T_s is the system time constant given by:

$$T_s = \frac{2\sum HS}{kP_{l0}} \quad (4)$$

$$\varphi = 1 - f/f_0 \text{ and } \delta_g = -g/kP_{l0} \quad (5)$$

Similarly, the frequency deviation resulted from a sudden loss of load *l* at time $t = 0$ can be expressed as:

$$\varphi = \delta_l \left(e^{\frac{-t}{T_s}} - 1\right) \qquad \text{for } t \geq 0 \quad (6)$$

where

$$\delta_l = l/[k(P_{l0} - l)] \quad (7)$$

If the frequency exceeds its normal operating band, the primary frequency control will be activated to ensure that the frequency is maintained within its short-term acceptable operating limits [17]. The primary control is often deployed within few seconds and provided by the generator governor response and automatic disconnection of interruptible load. Secondary control is deployed through Automatic Generation Control (AGC) within tens of seconds to minutes after the frequency disturbance occurs. It takes care of the remaining frequency deviation and brings the frequency back to its nominal value. Tertiary control provided by fast start-up generators is then manually deployed to replace the secondary control or complement it if the secondary control reserves are not sufficient for restoring the frequency [18].

Practically, each frequency control service has a particular shape of response such as a step response for load shedding or an exponential response for governor actions [19]. In this work, we assume that frequency control services can be modelled by a linear ramp response. This model has two advantages. Firstly, it is a simple technology neutral model, which can represent any real response with required accuracy. For example, a fast ramp approximates a step response, and a series of ramps of decreasing slope approximates an exponential response. Secondly, the levelling value of the ramp can represent the amount of the corresponding control service. A similar method has been used by Australian Energy Market Operator (AEMO) for dispatch of operating reserves deterministically [19].

Therefore, the complete frequency trajectory resulted from a loss of generation "g" occurs at time $t = 0$ with the participation of the power system frequency control modelled as a linear ramp response can be developed from (3) using the Laplace transformation technique. The result is

$$\begin{cases} \varphi = \delta_g \left(e^{\frac{-t}{T_s}} - 1\right) & \text{for } 0 \leq t \leq t_n \\ \varphi = \delta_g \left(e^{\frac{-t}{T_s}} - 1\right) - \dfrac{\delta_r \left[T_s\left(e^{\frac{-(t-t_n)}{T_s}} - 1\right) + t - t_n\right]}{T_r} & \text{for } t_n < t < t_n + T_r \\ \varphi = \delta_g \left(e^{\frac{-t}{T_s}} - 1\right) - \delta_r \dfrac{\left[T_s\left(e^{\frac{-(t-t_n)}{T_s}} - e^{\frac{-(t-t_n-T_r)}{T_s}}\right) + T_r\right]}{T_r} & \text{for } t_n + T_r \leq t \end{cases} \quad (8)$$

where $\delta_r = r/kP_{l0}$ with *"r"* is the amount of the frequency control service; t_n is the time when the frequency exceeds the normal operating threshold f_n resulting in the activation of the frequency control service. It can be determined by solving the equation below

$$\varphi(t_n) = \delta_g \left(e^{\frac{-t_n}{T_s}} - 1\right) = 1 - \frac{f_n}{f_0}; \quad (9)$$

T_r is the duration the frequency control service needs to reaches its maximum level *"r"* after its activation.

If at any time the frequency goes out of the acceptable operating limits, additional measures such as automatic under frequency load shedding (UFLS) need to be carried out to bring the frequency back within its limits. Using the frequency response model given by (8), we can determine whether and when the frequency exceeds the limits. If UFLS is activated, it will be modelled as a step change in load and using the same method we can develop the new frequency trajectory after the disconnection of load from (8).

For example, let us consider a loss of 200 MW generation occurring at time $t = 0$ in a 1000 MW system. The load relief factor is $k = 2$ and the system aggregate effective inertia after the loss of generation is 6000 MWs. The minimum frequency for normal operation is $f_n = 49.85\ Hz$. If the frequency exceeds this limit, the system fast frequency control service will be activated and fully deployed after 6 seconds. The amount of this service is r = 100 MW. There are two under frequency load shedding thresholds: $f_{x1} = 48.7$ Hz and $f_{x2} = 48.34$ Hz. The amount of load to be shed at each UFLS threshold is $l = 50\ MW$. Using the method presented above,

the activation time of the frequency control service will be t_n = 0.18 s, and the frequency deviation will trigger the two UFLS thresholds at t_{x1} =1.96 s and t_{x2} = 3.90 s, respectively.

III. Risk-based Assessment of Primary Frequency Response and Reserve Requirement

To evaluate the adequacy of primary frequency response (PFR), we use the risk assessment approach proposed in [15]. The PFR inadequacy risk is given by

$$Risk = \sum_j \sum_i P(C_i) \times P(S_j) \times Q(C_i, S_j) \quad (10)$$

where $P(C_i)$ is the probability of the ith contingency C_i, $P(S_j)$ is the probability of system operating condition S_j, and $Q(C_i, S_j)$ is the quantified consequence of the contingency C_i in the operating condition S_j.

To calculate the probability of random contingencies, it is assumed that the failure/repair cycle of a single unit is represented by a two-state Markov model and its transitions follow an exponential probability distribution. Thus, the probability of failure of a single component during a time period T, given that the repair process is neglected, can be expressed as [20]:

$$P(C_i) = 1 - e^{-\lambda_i T} \quad (11)$$

where λ_i is the failure rate of the given component.

In addition to random contingencies, power systems are subjected to unexpected variations in demand and power supply especially with the present of intermittent wind power generation. The load level at time t, l^t is the sum of the forecast load, l_f^t, and forecast error, ε_l^t. The load forecast error can be modelled as a zero-mean normally-distributed random variable with a standard deviation σ_l^t [6]:

$$\sigma_l^t = \frac{a}{100} l_f^t \quad (12)$$

where a is a constant representing the load forecast accuracy. Similarly, the wind generation level at time t, w^t, can be modelled as the sum of the forecast wind generation, w_f^t, and the forecast error, ε_w^t. As explained in [15], WPG forecast errors generally can be modelled as a normally-distributed random variable with zero mean and standard deviation σ_w^t which is given by:

$$\sigma_w^t = (\alpha + \beta \times w_f^t) W_I \quad (13)$$

where α and β are forecast parameters depending on the forecast horizon and the size of the region where wind farms are located, w_f is the forecast output of wind generation in per unit, and W_I is the total installed WPG capacity. To reduce computation time, instead of using the continuous normal probability distribution, the typical seven-interval discretization of the zero-mean continuous normal-distributed function is used. Therefore, at a given time t in the future, there are seven possible load levels and seven possible wind generation levels, and hence forty-nine possible operating conditions with the probability given by

$$P(S_{i,j}^t) = P(l_i^t) \times P(w_j^t) = P(\varepsilon_i) \times P(\varepsilon_j) \text{ for } i, j=1,...,7 \quad (14)$$

The consequence of a contingency in an operating condition is quantified by the amount of expected load interruption cost (ELIC), which is the product of the unit interruption cost (UIC) or value of lost load (VoLL) in \$/MWh and the expected energy not supplied (EENS) in MWh. The EENS is estimated based on the amount of unwanted load curtailments such as under frequency load shedding (UFLS) due to frequency deviations using the mathematical models of frequency developed in the previous section. Detail explanation is provided in [15].

After evaluating the adequacy of PFR, the resulted risk given by (10) will then be used to determine the primary reserve requirement by co-optimizing with energy in a security-constrained economic dispatch in order to minimize the expected operation cost (EOC) given by

$$EOC = CoE + Risk + CoPR \quad (15)$$

where *CoE* is the cost of energy – the product of energy price (\$/MWh) and energy demand (MWh); and *CoPR* is the cost of primary reserve – the product of reserve price (\$/MWh) and reserve demand (MWh).

IV. Case Study

A case study is performed to evaluate the performance of the proposed risk-based assessment method. The test case system S1 is a small islanded power system with characteristics similar to the Tasmanian power system. The total installed generation capacity of the system is 2.9 GW with 2.2 GW of hydro, 400 MW of gas, and 300 MW of wind generation. The power demand of S1 is approximately in the range of 800-1700 MW [21]. It is connected to a larger power system S2 (maximum demand 9000 MW) via a single monopolar HVDC link with a capacity to transfer maximum 500 MW of power and minimum 50 MW of power in both direction. The HVDC link is also equipped with a frequency controller allowing it to transfer frequency control services between the two systems subjected to the margins between its power flow and transfer limits.

Figs 1, 2 and 3 show the system hourly predispatch/ forecast data for the next 24 hours sourced from [22]. Due to specific characteristics of the predominantly hydro-power system and its small size, the capability of providing fast frequency response in S1 is limited resulting in high cost of primary reserve, as can be seen in Fig. 3. In contrast, the cost of the primary reserve in S2 is much lower due to the dominance of thermal generation units that represent much

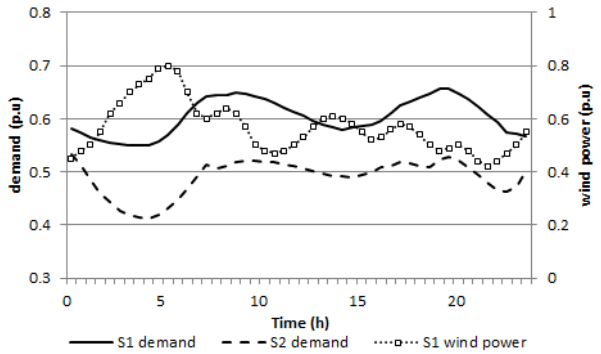

Fig. 1. Normalized forecast demand and wind power generation. The base values of S1 demand, S2 demand and S1 wind power are 1700 MW, 9000 MW and 300 MW, respectively.

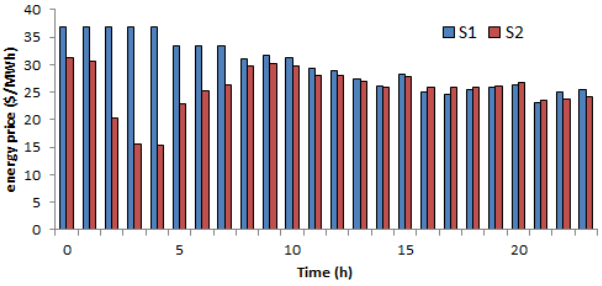

Fig. 2. Hourly forecast energy prices.

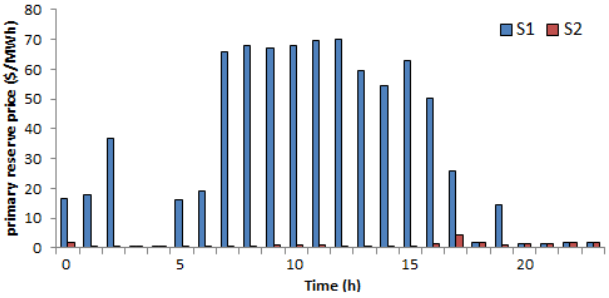

Fig. 3. Hourly forecast primary reserve prices.

cheaper sources of service in this system. In addition, the wind power generation level of S2 is negligible in comparison with the system size. The system inertia and capability of providing fast frequency responses are also strong. As a result, the reserve requirement for S2 is always set to the size of its largest online generator (550MW) and the PFR inadequacy risk of S2 is assumed to be negligible.

The study objective is to determine the interconnection flow (negative for import to and positive for export from S1) and the primary reserve requirement for S1 for each hour so that the operation cost of the two systems is minimized using the approach proposed in Section III. The results will then be compared with two other methods for primary reserve determination:

- Method A: $Reserve = P_{gen\_max}$, which is the size of the largest online generator.
- Method B: $Reserve = P_{gen\_max} + 3 \times \sigma_{netload}$ as proposed in [23] where $\sigma_{netload}$ is the standard deviation of net-load (demand minus wind generation) forecasting error given by

$$\sigma_{netload} = \sqrt{\sigma_l^2 + \sigma_w^2} \tag{16}$$

The contingency probabilities for S1 are calculated as explained in Section III. The failure rates of system components are determined based on the reliability data of the Tasmanian power network provided by TasNetworks. It is assumed that the failure probability of the interconnection link is zero. Load forecast errors are given by (12) with $a = 1$. Wind generation forecast errors are given by (13) with $\alpha = 0.01$ and $\beta = 0.16$ based on the data of 1-hour WPG forecast in a region with a diameter of 360 kilometres [24]. Due to the small size of the test system it is assumed that the wind speeds at all wind farms in S1 are the same at any given moment.

The system nominal frequency is 50Hz. The primary frequency control is activated once the system frequency drops below 49.85 Hz, and it take 6 seconds to reach its maximum value. This corresponds to the fast rise frequency control ancillary service (R6 FCAS) in Australia [25]. There are three under-frequency relay settings for the period of the primary control shown in Table I. These settings are similar to the automatic under-frequency load shedding configuration used in [26]. The load relief factor is $k = 1$. The unit interruption cost (UIC) is $12,500/MWh - the market price cap (MPC), which is often used in reliability studies in Australia [27]. Results are shown and analyzed in Section V.

V. Results and Discussion

A. Methods of Setting Reserve Requirements

In Fig. 4, we represent a comparison of the hourly dispatch outcomes in terms of the expected operation cost (EOC) for the next 24 hours obtained using the proposed optimized approach against Method A and Method B. As can be seen, the optimized approach provides the least expensive solution for all 24 hours and can save up to 1.5% of EOC compared to the other two methods. This saving is rather modest due to a number of reasons. Firstly, as the size of S2 is much bigger than S1, its cost of energy (CoE) accounts for more than 80% of the total EOC. Secondly, the saving is achieved by optimizing the primary reserve requirement and PFR inadequacy risk for S1 only, whereas the primary reserve amount of S2 is fixed and its PFR inadequacy risk is negligible as explained in Section IV. If the wind power generation level in S2 is large enough, the same optimization approach can be applied to S2 and bigger saving can be achieved. Meanwhile, Method A, which sets the primary reserve amount equal to the largest online generator, results in the most expensive solution in 15 hours.

Fig. 5 shows the hourly dispatch outcomes including the interconnection flow and the S1 primary reserve provision. As can be seen, the energy price plays an important role in determining the interconnection flow. For example, from hour 16 to 21 the interconnection flow is set to its maximum exporting level of 500 MW (S1 exports energy to S2) to take the advantage of cheaper energy prices in S1. At this level of export, S1 can also access lower cost source of primary reserve in S2 as the HVDC interconnection link can transfer up to 450 MW of reserve from S2 to S1. On the other hand, from hour 0 to 9, energy is imported from S2 to S1 as the energy price in S2 during this period is much lower than in S1. However, the amount of power imported might be limited to provide room for transferring reserve from S2 to S1 when needed as reserve price in S1 is often much higher than in S2. For example, during hour 2, the interconnection flow is set at 279.55 MW, 350 MW and 264.03 MW to provide room for 219.45 MW, 150 MW and 235.97 MW of reserve, respectively, using the optimized approach, Method A and Method B, respectively. In contrast, during the next two hours, 3 and 4, the interconnection flow is set to its maximum importing level of 500 MW (S1 imports 500 MW from S2) using any of the three approaches as the difference between the reserve prices in S1 and S2 is very small compared to the difference between the energy prices in the two systems.

However, in hour 15 the interconnection flow does not follow the sign of the difference in the energy prices. In this period, although the energy price in S2 is lower than in S1, the interconnection flow is set to be positive or in other words, S1 exports energy to S2. The reason is that during this period the difference in energy price between the two systems is very small while the cost of reserve and the PFR inadequacy risk in S1 are high.

Fig. 5 also shows that the reserve does not always need to cover the loss of the largest generator. For example, during hour 0 and 2, the optimized reserve amounts for S1 are 39.02 MW and 47.93 MW, respectively. The reason is that during these periods, the cost of providing primary reserve in S1 is higher than the benefit of having additional reserve. In contrast, in a number of cases, such as from hour 7 to 13, the S1's primary reserve is set very close to its maximum value to reduce the system PFR inadequacy risk.

TABLE I.
UNDER-FREQUENCY RELAY SETTINGS

Relay	Load shedding block size (%)	Frequency threshold 1 (Hz)	Time delay 1 (s)	Frequency threshold 2 (Hz)	Time delay 2 (s)
1	10	47.8	0.2	-	-
2	10	47.5	0.2	47.8	10
3	10	47.2	0.2	47.5	2

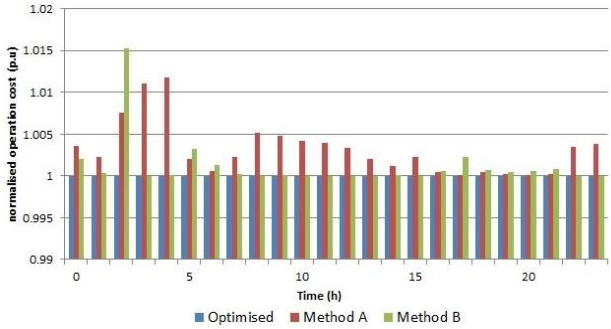

Fig. 4. Hourly expected operation costs obtained with the three approaches. These costs have been normalized based on the expected cost obtained with the proposed optimized approach.

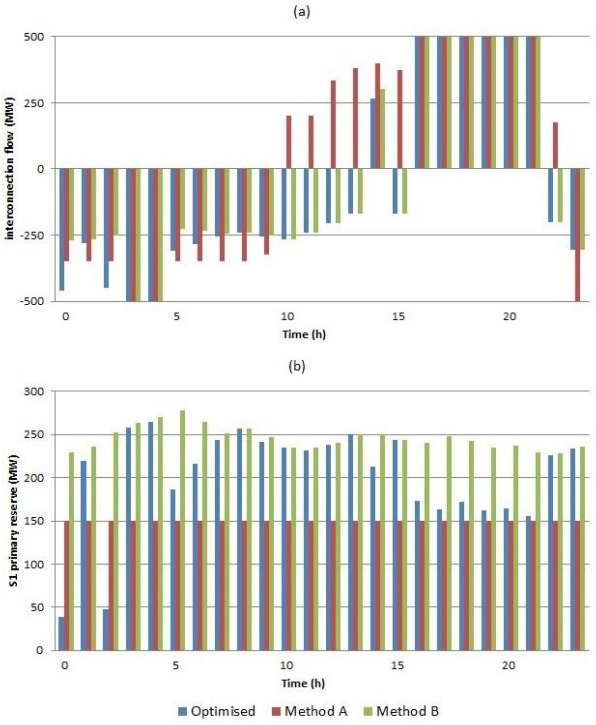

Fig. 5. (a) Interconnection flows and (b) S1 primary reserve provisions obtained with the three approaches.

B. *Impact of the Installed Wind Power Capacity*

Fig. 6 shows how the total expected cost of operation for the next 24 hours obtained with the optimized approach varies as a function of the installed wind power capacity. It is assumed that the pre-dispatch data are still the same while the installed capacity varies. These results show that the total operation cost increases as the installed capacity increases. This is a rather expected result as higher installed wind power capacities would lead to higher wind forecasting errors, and hence to higher system uncertainty. This may also reduce the number of synchronous generators online leading to a decrease in system inertia. As a result, the system PFR

inadequacy risk increases and a larger reserve provision is required, as can be seen in Fig. 7.

However, we should note that with the higher installed wind power capacity, the energy price may drop, and a hence lower operation cost might be achieved. Additional wind power generation also reduces CO_2 emissions, which in turn, could be translated into additional economic benefits.

C. *Impact of the System Inertia*

After a frequency deviation occurs, rotating machines in a power system immediately release their kinetic energy to arrest the change in frequency. This is called inertial responses. The total system inertia plays an important role to limit RoCoF as well as frequency nadir. Increasing integration of non-synchronous converter-based generations such as WPG may reduce the inertial response leading to an increase in RoCoF, leaving insufficient time for PFR to deploy and arrest frequency deviations. If RoCoF is high enough, it can trigger the generator's RoCoF protection tripping additional generators, which in turn increases the severity of the frequency deviation, and may lead to the system blackout.

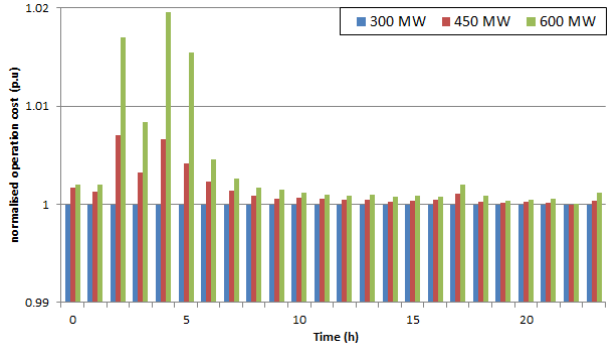

Fig. 7. Hourly expected operation costs obtained with the proposed optimization approach for three different levels of installed wind power capacity. These costs are normalized with the base cost = cost associated with the case having 300 MW of installed wind power.

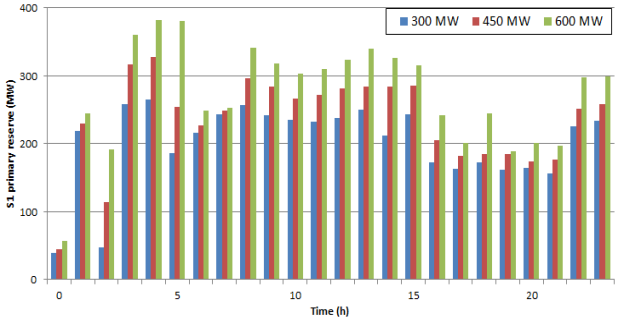

Fig. 8. Variation of S1 primary reserve provision as a function of the installed wind power capacity.

Low inertia also increases the phase shift during system disturbances, which in turn may affect operation of power electronics in particular operation of line commutated converters and phase lock loop (PLL) oscillators with the consequential impact on power generation or HVDC transmission. Therefore, it is important to secure a sufficient provision of system inertia. Fig. 8 shows how the total expected cost of operation for the next 24 hours obtained with the optimised approach varied as a function of the system inertia. A minimum level of inertia is secured for each case. In this study, we do not consider the cost of inertia. As can be seen, the operation cost reduces as the minimum system inertia increases.

In reality, increasing inertia incurs costs. In order to increase power system inertia, we can either operate generators on low load mode or dispatch synchronous condenser units to the grid. The former method may result in the generators operating away from their efficient rating, which leads to an increase in generation (fuel) cost. It may also increase the maintenance cost and reduce a plant's lifecycle as it may not have been designed for prolonged operation at low loading. The latter method incurs the cost of running synchronous condensers including energy drawn from the grid and maintenance cost. However, at present no electrical power system in the world has implemented a market or incentive-based rewards for providing inertia service
[28].

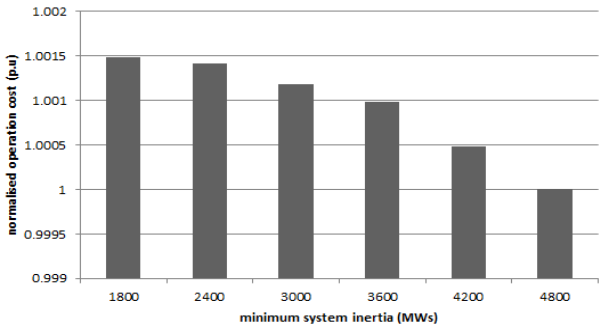

Fig. 9. Variation of the total expected operation cost for the next 24 hours as a function of the minimum system inertia. These costs are normalized with the base cost = cost associated with the case of 4800 MWs inertia.

Although converter-based wind turbines have no inherent inertial response, they are capable of injecting more active power into the grid using their converter controller in frequency deviation events. There are two types of frequency responses a wind turbine can provide: synthetic inertial and governor-like (frequency droop) responses. The former utilizes the kinetic energy stored in the wind turbine (i.e., generator, gearbox and blades). The release of kinetic energy from a wind turbine can be controlled independently from the RoCoF. In theory, it can even deliver a larger inertial response than a traditional synchronous generator. This is a highly desirable characteristic especially for small power systems with limited capacity to supply frequency control ancillary services. In these systems, WPG can provide fast frequency support in the first few seconds after a frequency disturbance occur to improve RoCoF and to buy time for other generators

to respond through their governor systems. In predominantly hydro-power systems, this may compensate for the initial reduction in power output, which is caused by pressure reduction due to opening of the wicket gate during the first few seconds [29]. However, if the wind turbine is operating below its rated wind speed, there will be a recovery period in which the turbine power output needs to be reduced for the turbine re-acceleration [30]. Thus, achieving a governor-like wind turbine response requires the turbine to be operated at a power output, which is lower than the output that can potentially be achieved at a given wind speed (wind power curtailment). This means that the turbine needs to operate at a sub-optimal operating point, which represents additional costs that need to be considered. Further studies are required to assess the benefits of the frequency response of wind turbines as well as potential consequences before it can be widely implemented in power system operating schemes and considered in new ancillary service market designs.

VI. CONCLUSION

The paper presented a risk-based stochastic approach to assessing the adequacy of primary frequency response, and determining the primary reserve requirement taking into account wind power generation and load forecast uncertainties. The amount of primary reserve provision is determined so that the total system expected operation cost (i.e., the sum of the actual operating cost and the risk of primary frequency response inadequacy in terms of load interruption cost) is minimized. A mathematical model of frequency responses is developed to dynamically evaluate the primary frequency response without running dynamic simulations. A case study is performed to demonstrate the performance of the proposed approach. The results show that the risk-based approach has potential to deliver lower cost dispatch solution compared with the traditional method setting the reserve requirement based on the largest generator infeed and a combination of loss of the largest generator and the net load uncertainty. The proposed approach is also able to assess the impact of the installed wind power capacity and the total system inertia on the expected cost of operation.

REFERENCES

[1] T. Acker, "IEA Wind task 24 - Integration of wind and hydropower systems," NREL, Dec. 2011.

[2] D. Jones, S. Pasalic, and M. Negnevitsky, "Determining the frequency stability boundary of the Tasmanian system due to voltage disturbances," in Proc. IEEE POWERCON, Auckland, NZ, 2012, pp. 1-6.

[3] Electric Power Research Institute (EPRI), "Frequency response adequacy and assessment: Global industry practices and potential impact of changing generation mix," Dec. 2012.

[4] F. Bouffard and F.D. Galiana, "Stochastic security for operations planning with significant wind power generation," IEEE Trans. Power Syst., vol. 23, no. 2, pp. 306-316, May 2008.

[5] M. A. Matos and R. J. Bessa, "Setting the operating reserve using probabilistic wind power forecasts," IEEE Trans. Power Syst., vol. 26, no. 2, pp. 594-603, May 2011.

[6] M. A. Ortega-Vaquez and D. S. Kirschen, "Estimating the spinning reserve requirements in systems with significant wind power generation penetration," IEEE Trans. Power Syst., vol. 24, no. 1, pp. 114-124, Feb. 2009.

[7] G. Dany, "Power reserve in interconnected systems with high wind power production," in Proc. IEEE Power Tech. Conf., Porto, Portugal, Sep. 2001.

[8] S. Persaud, B. Fox, and D. Flynn, "Effects of large scale wind power on total system variability and operation: Case study of Northern Ireland," Wind Engineering, vol. 27, pp. 3-20, 2003.

[9] R. Doherty and M. O'Malley, "A new approach to quantify reserve demand in systems with significant installed wind capacity," IEEE Trans. Power Syst., vol. 20, pp. 587-595, May 2005.

[10] M. Black and G. Strbac, "Value of bulk energy storage for managing wind power fluctuations," IEEE Trans. Energy Conversion, vol. 22, pp. 197-205, Mar. 2007.

[11] M. A. Ortega-Vaquez and D. S. Kirschen, "Assessing the impact of wind power generation on operating costs," IEEE Trans. Smart Grid, vol. 1, no. 3, pp. 295-301, Dec 2010.

[12] A. Papavasiliou, S.S. Oren, and E.P. O'Neill, "Reserve requirements for wind power integration: A scenario-based stochastic programming framework," IEEE Trans. Power Syst., vol. 26, pp. 2197 - 2206, 2011.

[13] M. Vrakopoulou, K. Margellos, J. Lygeros, and G. Andersson, "A probabilistic framework for reserve scheduling and N-1 security assessment of systems with high wind power penetration," IEEE Trans. Power Syst., vol. 28, pp. 3885-3896, Nov. 2013.

[14] H. Chavez and R. Baldick, "Inertia and governor ramp rate constrained economic dispatch to assess primary frequency response adequacy," in Proc. Int. Conf. Renewable Energies and Power Quality, 2012

[15] M. Negnevitsky, D. H. Nguyen, and M. Piekutowski, "Risk assessment for power system operation planning with high wind power penetration," IEEE Trans. Power Syst., to be published.

[16] A. J. Wood and B. F. Wollenberg, Power generation, operation and control. New York, US: Wiley, 1996.

[17] North American Electric Reliability Corporation (NERC), "Balancing and frequency control," 2011.

[18] UCTE Operation Handbook - Policy 1: Load-Frequency Control and Performance, 2004.

[19] National Electricity Market Management Company (NEMMCO), "Dispatch of contingency frequency control ancillary services," Dec. 2003.

[20] R. Billinton and R. Allan, Reliability evaluation of power systems, 2 ed., 1996.

[21] Transend Network, "Transend annual planning report 2013," Australia, 2013.

[22] Australian Energy Market Operator (AEMO) Data. Available: www.aemo.com.au/Electricity/Data.

[23] V. Silva, "Value of flexibility in systems with large wind penetration," Ph.D. dissertation, Imperial College London, University of London, London, UK, 2010.

[24] A. Fabbri, T. G. S. Roman, J. R. Abbad, and V. H. M. Quezada, "Assessment of the cost associated with wind generation prediction errors in a liberalized electricity market," IEEE Trans. Power Syst., vol. 20, no. 3, pp. 1440-1446, Aug. 2005.

[25] B. Blake, "ESOPP guide - FCAS constraint equations," Australian Energy Market Operator (AEMO), Dec. 2009.

[26] K. Mollah, M. Bahadornejad, and N. Nair, "Automatic under-frequency load shedding in New Zealand power system — A systematic review," in Proc. 21st AUPEC, Brisbane, QLD, Australia, Sept. 2011, pp. 1-7.

[27] AEMC Reliability Panel, "Final report: Reliability standard and reliability settings review," Australian Energy Market Commission, 2010.

[28] J. Riesz and I. MacGill, "Frequency control ancillary services - Is Australia a model market for renewable energy," presented at the 12th International workshop on large-scale integration of wind power into power systems, London, Oct. 2013.

[29] US Bureau of Reclamation, "Mechanical governors for hydroelectric units - Facilities, instructions, standards, and techniques," Jul. 2002.

[30] Electric Reliability Council of Texas (ERCOT), "Future ancillary services in ERCOT," 2013.

.